描述通風溫室中二氧化碳濃度動態之線性控制模式

A Linear Control Model Describing the Dynamics of Carbon Dioxide Concentrations in A Ventilated Greenhouse

國立宜蘭農工專校農機科副教授　國立臺灣大學農工系副教授　國立臺灣大學農工系教授

廖中明　王鼎盛　劉佳明

C. M. Liao　T. S. Wang　C. M. Liu

摘　要

由團塊參數近似法觀點所推導出之線性控制模式可描述通風溫室中任一點二氧化碳濃度之動態行爲。系統方程式可以第一階非時變之向量一矩陣微分方程式表示。計畫中並設計一環境氣候箱實驗以評估團塊參數模式預測通風空間中二氧化碳濃度的準確性。二氧化碳濃度的特性是藉量測環境氣候箱中在一廣泛範圍通風率下之平衡濃度。二氧化碳濃度暫態反應之評估則是觀測以通風量爲函數之三點濃度變化爲主。模式的數值解是以三度空間團塊形式之控制體積其氣流率之守恆關係而得。模式鑑定結果顯示量測二氧化碳濃度值與團塊參數模式所得之預測值相吻合（偏差值爲8％）。在低通風率狀況下，量測值與預測值之差異則較大（偏差值爲13～14％）。

關鍵詞：二氧化碳，通風溫室，動態行爲，團塊參數模式，環境氣候箱，線性控制模式。

ABSTRACT

A linear control model for describing the dynamic behavior of carbon dioxide concentration at any location within a ventilated greenhouse is presented from the standpoint of a lumped-parameter approximation. The system equation can be represented by a first-order time-invariant vector-matrix differential equation. To assess the accuracy of a lumped-parameter model used in predicting carbon dioxide concentrations in a ventilated airspace, a laboratory project is presented. The carbon dioxide concentration was characterized in an environmental chamber by measuring its equilibrium concentrations over a range of ventilation rates. The transient behavior response of carbon dioxide concentrations was evaluated at three points and monitored as a function of ventilation rate. The model calculation solved as a three-dimensional lumped form of control volumes representing conservation of air-flow rate. Good agreement was obtained between measured carbon dioxide concentrations and those predicted by the lumped-parameter model (deviation was 8%), however at low ventilation rates, some disagreement between predicted and measured results occurred (deviations were 13-14%).

Keywords: carbon dioxide, ventilated greenhouse, dynamic behavior, lumped-parameter model, environmental chamber, linear control model.

1. INTRODUCTION

Whenever a greenhouse contains plants with green leaves there will be an increasing deficit of CO_2 concentration as irradiance increases. If the rate of ventilation was low, the effect was dramatic (Saffell and Mattews, 1983). At the elevated temperature required for growing tropical crops in greenhouses, there was generally little ventilation and, therefore the need for increasing CO_2 to prevent reduction in the rate of photosynthesis. At least, CO_2 was injected to maintain its concentration inside the greenhouse similar to that outside, a system of control also enable computation of the net rate of assimilation of CO_2 by the stands within a ventilated greenhouse.

The CO_2 concentration disperse throughout a ventilated greenhouse is a complex manner, that depends on the nature of an airflow into, out of, and within the greenhouse system, that depends on the possibility of chemical reaction, or sorption of CO_2.

A distributed-paraameter model represented by the Navier-Stokes equation that describes airflow system in a ventilated airspace takes the form of partial differential equations (Landau and Lifshitz, 1987). These are moe difficult than ordinary differential equations to solve, both analytically and numerically. On the other hand, in a three-dimensional flow system in a ventilated airspace, the meaning of some of the system coefficients in equations such as turbulent diffusivities is not always clear. However, a distributed-parameter process can still be considered when using a lumped-parameter approximation.

To illustrate this point, a ventilated airspace may be considered in which CO_2 concentration, C at any distance $\vec{r}(x,y,z)$ is a function of time t. Thus $C=C(\vec{r},t)$. The most accurate model for $C(\vec{r},t)$ would involve both spatial and temporal derivation and would be described by a partial differential equation. Rather than formulating this model, the ventilated airspace can be approximated by a number of "lumps", each having its own representative CO_2 concentration, which are assumed to be constant throughout the lump, i.e., $C(\vec{r},t)=C(t)$. A lump, here, is small relative to the scale of the system but larger relative to the molecular scale and its state is defined by its temperature, pressure, local airflow rate, and CO_2 concentration – the state-space analysis. The response of lumped-parameter model will approach the actual behavior as the number of lumps is increased.

The total airflow rates are assumed to occur at the interfaces of each lump. Total airflow rates include the internal secondary air circulation which may be generated by various heat sources, by temperature gradients, or by entrainment of air into the jet stream from the supply air duct. Therefore, it is possible to assume that CO_2 concentration in a ventilated airspace is similar to a box filled with turbulence with almost no net flow rate. The net flow rate at which CO_2 concentration will be transported can not be easily determined from air velocity measurements.

In this work a mathematical model will be formulated which will adequately describe the behavior of CO_2 concentration and account for its spatial changes in physical dynamics of the interior environment. To completely describe the local transport phenomena of CO_2 in a ventilated airspace, an environmental chamber was designed and constructed. The chamber had a volume of 1.35 m^3 (1.54x0.92x0.95 m). therefore, a labroatory project to assess the assuracy of a lumped-parameter model is presented. Verification of the model included the average equilibrium carbon dioxide concentration as a function of ventilation rate, and time-dependent carbon dioxide concentration at a designed location (or lump).

2. OBJECTIVES

In specific terms, the purposes of this paper

are:

(1) To model the dynamic behavior of CO_2 concentration that comprehensively and systematically accounts for complex transport process.

(2) To verify the lumpd-parameter model by using an environmental chamber for predicting CO_2 concentration based on CO_2 generation rates.

3. MODEL ASSUMPTIONS

Before deriving a set of system equations to describe the dynamic behavior of CO_2 concentration in a ventilated airspace from the viewpoint of lumped-parameter approximation, the following assumptions are made.

(1) Finite lump model. There are N lumps with $N \geqslant 1$.

(2) Ventilation air transport system. A flow rate $Q_{ij} \geqslant 0$ gives the airflow from the j^{th} to the i^{th} lump for $i \neq j$ with $1 \leqslant i, j \leqslant N$. A flow rate Q_{is} gives the input flow and a flow rate Q_{ei} gives the output flow rate for the i^{th} lump for $1 \leqslant i \leqslant N$.

(3) Airflow transfer system. A transfer flow rate Q_{ij} assumed to be entirely generated by entrainment air into the jet stream from the supply air duct. Therefore, the transfer airflow rate occurs at interface of the lump can be expressed as $Q_{ij}=F_{ij}(\beta)Q$, in which $F_{ij}(\beta)$ is the function of entrainment ratio (β) and can be calculated by the entrainment theory for air jets (ASH-RAE, 1985), and Q is the total volumetric flow rate of outdoor air supplied to the whole system.

(4) The carbon dioxide concentrations are dynamically passive, i.e., no chemical reaction between primary CO_2 concentration and normal atmospheric condition, and the motion of CO_2 totally dependents on the local airflow motion.

(5) The uniform mixing state in an airspace is in the sense of local meaning but not of global meaning.

(6) All physical quantities computed from the model represent the ensemble properties, i.e., it assumes that the process of model verification presupposes an ergodic hypothesis.

4. MODEL DEVELOPMENT

4.1. General formulation

As shown in Figure 1, a ventilated airspace can be divided into N arbitrary lumps. In each lump, the mixing is assumed to be uniform and instantaneous. Figure 1 shows that a time-dependent net CO_2 exchange rate, m(t), is a system-derived exchange rate by the mechanisms of photosynthesis, photolysis, and biological activity of soil microorganisms (Monteith, 1963; Noggle and Fritz, 1976). The net CO_2 exchange rate in the ventilated airspace is assumed to be instantaneous dispersed throughout the system. The population-balance model (Himmelblau and Bischoff, 1968) is the basic model for such a system describing the time-dependent change in CO_2 concentration. Therefore, with the above model assumptions, the population-balance equation for an arbitrary lump i in Figure 1 can be expressed as follows:

$$V_i dC_i(t)/dt = -Q_{ii}C_i(t) + \sum_{\substack{j=1 \\ (j\neq i)}}^{N} Q_{ij}C_j(t) + Q_{is}C_s(t) + m_i(t) \qquad (1)$$

where:

Q_{ii} = overall volumetric airflow rate leaving lump i, m^3/hr,

Q_{ij} = transfer airflow rate from lump j to lump i, m^3/hr,

$C_i(t)$ = CO_2 concentration leaving lump i, ppm,

$m_i(t)$ = time-dependent CO_2 net exchange rate in lump i, g/hr,

V_i = air volume of lump i, m^3,

Q_{is} = supplied airflow rate from outdoor to lump i, m^3/hr,

$C_s(t)$ = CO_2 concentration of supplied air, ppm.

By using the standard matrix notation (Hadley, 1961) to the whole system, equation (1) can be expressed as a general form:

$$[V]\{C(t)\} = -[Q¼]\{C(t)\} + [Q_s]\{C_s(t)\} + \{m(t)\} \qquad (2)$$

Where $\{C(t)\}$ is the time derivative of $\{C(t)\}$. Matrices [V], and $\{Q_s\}$ are diagonal matrices. Vectors $\{C(t)\}$, $\{C_s(t)\}$, and $\{m(t)\}$ are

column vectors with non-negative elements. Matrix [Q] is a square airflow matrix with entries Q_{ij}, where:

$$Q_{ij} = \begin{cases} -Q_{ij} \text{ for } i \neq j \\ \sum_{\substack{i=1 \\ (i \neq k)}}^{N} Q_{ki} \text{ for } i = j \end{cases} \quad (3)$$

Therefore, for the i^{th} row of [Q] the off-diagonal entries represent the airflow rates into the i^{th} lump from other lumps with negative sign, while the diagonal entries give the total airflow out of the i^{th} lump. With the model assumptions, the airflow matrix [Q] also can be expressed as:

$$[Q] = [\beta]\, Q \quad (4)$$

where $[\beta]$ is a square entrainment ratio function matrix with positive diagonal and negative off-diagonal values.

In view of equation (2], matrices [Q] and [V] also referred to as the system transport matrix and system volume martix, respectively. It obvious that $[V]^{-1}$ exists. Therefore, multiplying both side of equation (2) by $[V]^{-1}$, yields:

$$\{\dot{C}(t)\} = -[A]\{C(t)\} + [V]^{-1}\{m(t)\} + [D]\{C_s(t)\} \quad (5a)$$

where:

$$[A] = [V]^{-1}[Q] \quad (5b)$$

$$[D] = [V]^{-1}[Q_s] \quad (5c)$$

In view of equation (5a), the matrix [A] sometimes referred to as the system state matrix, conains the essential dynamic characters of the system being studied. Therefore, the dynamic behavior of CO_2 concentration in a ventilated greenhouse can be represented by a first-order time-invarient vector-matrix differential equation.

4.2. General solution

Linear dynamic equation (5a) may be rewritten as follows:

$$[Q]\,[\dot{C}(t)] + [V]\,[C(t)] = L(\{C(t)\}) = [E(t)] \quad (6a)$$

where:

$$\{E(t)\} = \{m(t)\} + [Q_s]\{C_s(t)\} \quad (6b)$$

L(.) in equation (6a) is a linear transformation operator and has the form of a linear transformation:

$$L([y(t)]) = [a]\{y(t)\} + [b]\{\dot{y}(t)\} + [c]\{\ddot{y}(t)\} + \ldots\ldots, \quad (7)$$

In view of equation (6a), $\{E(t)\}$ may be referred to as the system excitation vector. Therefore, the system is seemed to be driven by the system excitation, $\{E(t)\}$, that includes both net CO_2 exchange rates and supplied air CO_2 concentration, which, in general, vary with time.

The general solution of equation (6a) subjected to the initial condition, $\{C(t=0)\} = \{C(0)\}$, is (Chen, 1984):

$$\{C(t)\} = exp(-[A]\,t)\{C(0)\} + \int_0^t exp(-[A](t-\tau))[V]^{-1}\{m(\tau)\}d\tau + \int_0^t exp(-[A](t-\tau))[D]\{C_s(\tau)\}d\tau \quad (8)$$

where to and τ are any specific times.

In a specific case of constant CO_2 exchange rate vector ($\{m(\infty)\}$) and constant supplied CO_2 concentration vector ($\{C_s(\infty)\}$), the CO_2 concentration in equation (8) can be calculated as follows:

$$\{C(t)\} = exp(-[A]\,t)(\{C(0)\} - [Q]^{-1}\{E(\infty)\}) + [Q]^{-1}\{E(\infty)\} \quad (9)$$

The equilibrium CO_2 concentration vector attained is given by:

$$\{C(\infty)\} = [Q]^{-1}\{E(\infty)\} \quad (10)$$

From the theory of matrices, the eigenvalues of $[A]^{-1}$ are equal to the riciprocal of the eigenvalues of $[A]$. Therefore, when $[A]^{-1}$ has j different eigenvalues (complex eigenvalues will always occur in conjugate pairs since the elements of $[A]^{-1}$ are real), then equation (10) can be expressed in a more explicit form as:

$$\{C(t)\} = \sum_{k=1}^{j} a_k \exp(1/\lambda_k t)\{\chi^{(k)}\} + [C(\infty)] \quad (11)$$

where:

a_k = constant coefficients, dependent on the initial conditions,

λ_k = system eigenvalues of $[A]^{-1}$,

$\{\chi^{(k)}\}$ = eigenvector of $[A]^{-1}$ corresponding to λ_k.

5. EXPERIMENTAL PROCEDURES AND EQUIPMENT

The test facilities used in the experimental studies were comprised of (1) an environmental chamber, (2) an air delivery system, (3) a carbon dioxide gas generating system, and (4) a carbon dioxide gas sampling and analyzing system. The ambient temperature during experiment was 30-32°C. The relative humidity ranged between 70% and 80%.

Environmental chamber

The dimensions and general outline of the environmental chamber are given in Figure 2. The dimensions were 1.54x0.92x0.95 m, for a volume of 1.35 m^3. The dimension were such as to simulate one ventilated greenhouse with an negative pressure ventilation system. The chamber, fabricated from one plexiglass and three sandwich-type boards, had a small 16 cm diameter fan located on the floor of the chamber for maintaining uniform mixing of the CO_2 concentration throughout the chamber.

Air Delivery system

The air entered the chamber through a long slot (92x4.5 cm) inlet. A 30 cm diameter, 6-blade propellor fan was used to exhaust air from the chamber. The exhaust location was 85 cm from floor level measured to the center of the outlet. The fan operated at constant speed by a voltage indicator to try to maintain a constant air velocity over the all sampling. The fan output (m^3/hr) was measured near the end of a discharge duct. To ensure that the circulating airflow in the chamber was trubulent flow, good air mixing within the chamber was demonstrated by using a smoke to visualize the airflow pattern. Smoke density quickly became uniform in the chamber and there almost appeared to be no stagnant spots. Ventilation rates used throughout the experiment were 371, 851, and 1070 m^3/hr, respectively.

Gas generating system

Gas generating system consisted of a high pressure cylinder of carbon dioxide, a two-stage pressure regulator, plastic tubing, and three HSIN CHUAN flowmeter (M-type, Catalog No. HC-A02)(Figure 2). Discharge from the cylinder of pure carbon dioxide was divided into three for the generating operation. The HSIN CHUAN M-type flowmeter had a millimeter scale which could be converted to a volume flow scale for air with aid of calibration charts. Adjustment factors associated with the calibration charts were used to calculate the gas flow rate for gases other than air. According to manufacturer's information the adjustment factor is equal to the square root of the specific gravity of air divided by the specific gravity of carbon dioxide. The value is equal to 0.818. The carbon dioxiode was used at a rate of 500 1/hr.

In order to investigate the variation of carbon dioxide concentration influenced by the location of generation sources, the carbon dioxide generating points were layout as shown in Figure 3. Figure 3 shows that the carborn dioxide generating points were below the sampling points 7, 10, and 11 as denoted by m_7, m_{10}, and m_{11}, respectively.

Gas sampling and analyzing systems

Measurement of carbon dioxide concentration were obtained by two KRK Model 200-type CO_2 meters (Kasahara Chemical Instru-

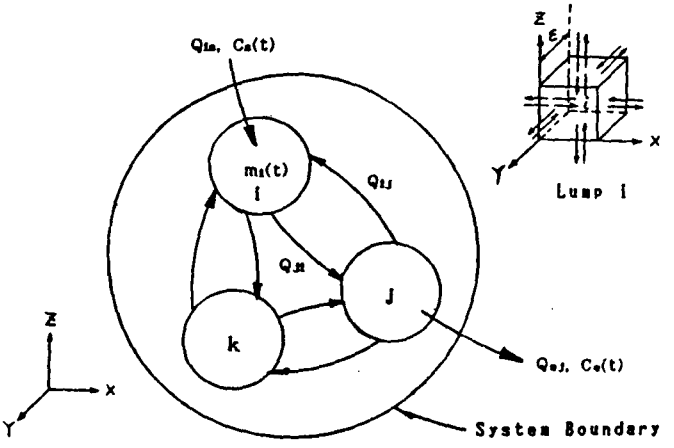

Figure 1. Schematic diagram of a lumped-parameter model and a control volume i of a slot-ventilated airspace.

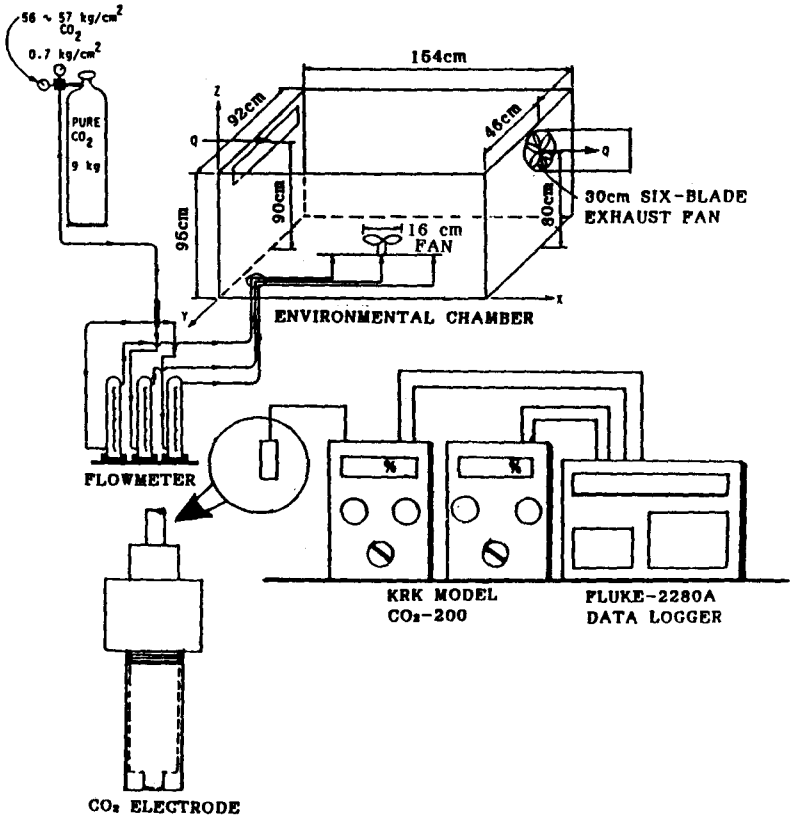

Figure 2. Layout of experimental equipment and the dimension of environmental chamber.

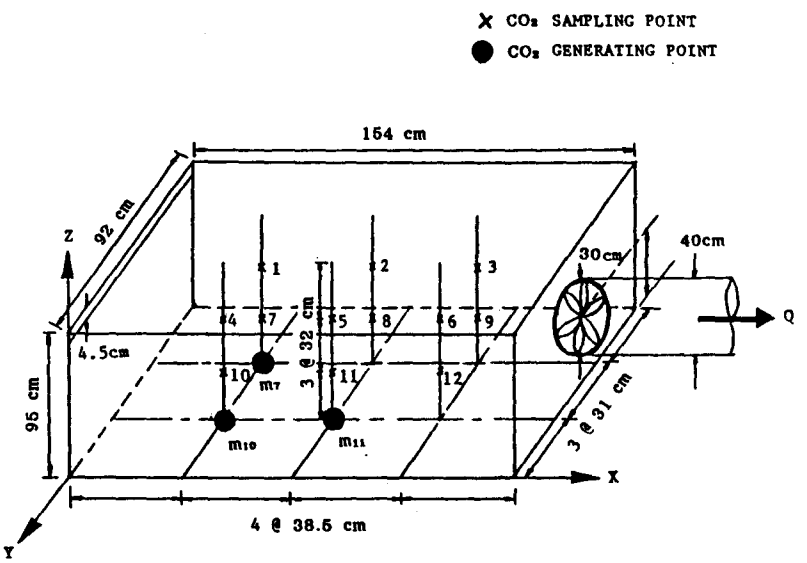

Figure 3. A general outline of the environmental chamber showing the locations of sampling point and carbon dioxide generating point.

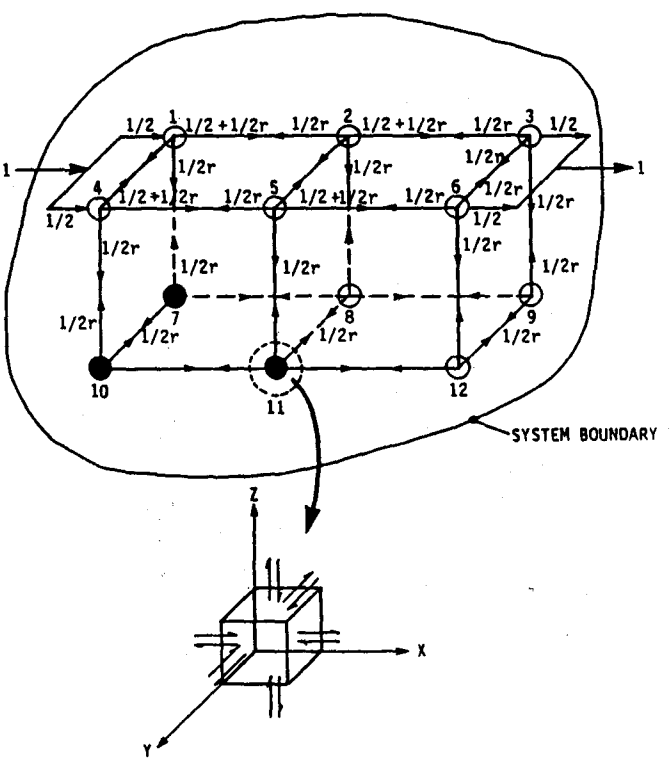

Figure 4. Airflow patterns and control volume used in model verification ($r = \beta$ = entrainment ratio).

ments Corp., Japan). The measuring principle for those two CO_2 meters is based on the potentiometric methods: carbon dioxide gas passed into membrane of the electrode system in contacting with $NaHCO_3$ solution results in a change of PH value. Carbon dioxide concentration thus can be measured through the potential difference derived from the proportional relationship between the change of PH value and partial pressue of carbon dioxide gas. Before the chamber test, both two CO_2 meters were calibrated with known CO_2 concentrations of 0% and 10%, respectively (Kasahara Chemical Corp., Japan). To detect concentration variations in both the longitudinal and vertical direction, sampling was carried out in two plans, 30.7 cm and 61.4 cm from a side wall (along y-direction in Figure 3). A total of 12 sampling points were chosen (Figure 3). The sampling outputs were read from a Fluke-2280A Data Logger (John Fluke MFC CO. Inc., U.S.A.). Equilibrium normally occur 60-70 minutes after constant carbon dioxide concentration was reached in the exhaust air. Sampling points 2 and 11 as well as outlet were chosen to study transient response of carbon dioxide at a sampling interval of 10 seconds. Sampling of the 12 points was carried out in random order and two subsample readings were made at each sampling point for studing their equilibrium responses.

6. PROCEDURES OF MODEL VERIFICATION

The lumped-parameter model for the environmental chamber is shown schematically in Figure 4. The x-y-z coordination of the environmental chamber was divided into 12 lumped form of control volumes. The control volume P in Figure 4 is a typical 3-D lumped form in the whole system in which its representative carbon dioxide concentrations undergoing local airflow rate transportation. Assume, for simplicity, that the primary airflow and circulating airflow are directed in the x-, y-, and z- directions. The basic input information for the model verification can be stated as follow.

(1) Entrainment ratio, β. The lower bound for entrainment ratio is much greater than 1. The actual value depends to some extend on the relative position between the supply and size, shape (circular or slot, etc.) of the nozzle or air jet, etc. Some estimations of the entrainment ratio are possible on the basic of a simple entrainment concept. It has been assumed that the secondary airflow, βQ, in a ventilated airspace is entirely induced by the primary airflow rate, i.e., by the entrainment in the inlet jets. Equation for the entrainment of jets from long slot has been mathematically presented in ASHRAE Handbook of Fundamentals (1985):

$$\beta = \beta Q/Q = \textit{entrained flow/initial flow}$$

$$= \sqrt{(2/K')\,(\chi/H_o)} \qquad (12)$$

where:

K' = proportionality constant, approximately 7,

X = distance from faces of outlet, cm, and

H_0 = width of slot, cm.

In this case, the air entered the environmental chamber through a 95x4.5 cm long slot. Therefore, the value of the entrainment ratio is euqal to 3.13.

(2) Airflow matrix, [Q]. The general entrainment ratio function matrix $[\beta]$ for the 12-lump model indicated in Figure 4 is list in Figure 5. Input data of the airflow are followed by equation (3) and (4) as well as the airflow patterns which are shown schematically in Figure 4. Figure 4 indicates that the solution of the airflow matrix is by 3-D lumped form of control volumes representing the conservation of airflow rates. Figure 5 indicates that airflow matrix [Q] is quasi-diagonally dominant, then [Q] is nonsingular (Liao and Feddes, 1990). This implies that $[Q]^{-1}$ exists. Furthermore, by a theorem on M-matrices (Plemmons, 1977), [Q] is an nonsingular M-matrix.

(3) Diagonal air volume matrix, [V]. In this model verification, the air volume of each lump is assumed equal, i.e., $V_1 = V_2 = \ldots = V_{12} = 0.11\ m^3$.

(4) Equilibrium CO_2 generation rate vector, $\{m(\infty)\}$. Total equilibrium CO_2 generation rate is 500 l/hr which is equal to 1065 g/hr (the

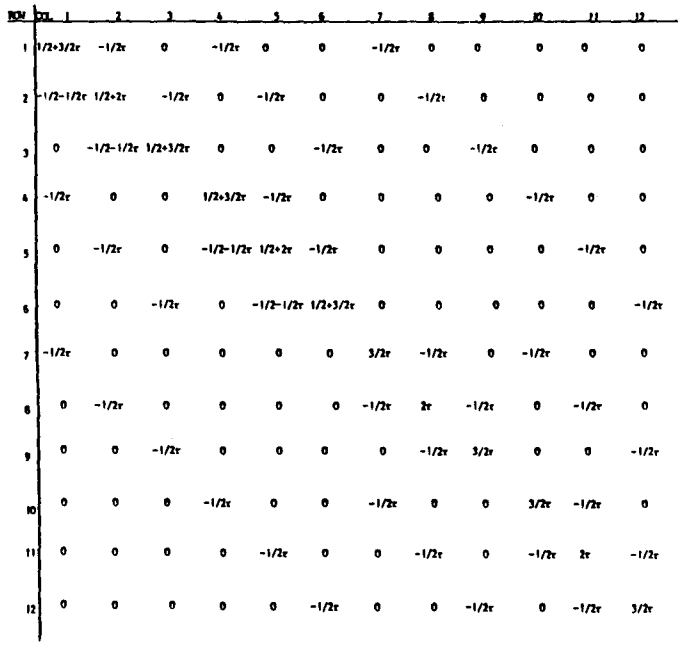

Figure 5. General entrainment ratio function matrix in the case of comparison with environmental chamber experiment ($r = \beta$ = entrainment ratio).

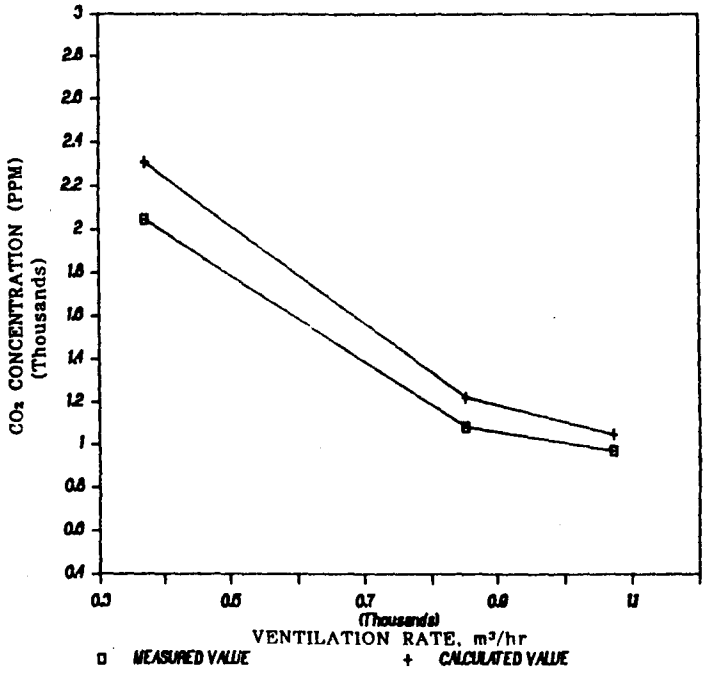

Figure 6. Comparison of measured mean carbon dioxide concentration and predicted results for different ventilation rate levels.

ambient air condition assumes under 30°C, 1 atm). Carbon dioxide generating points were below the sampling points 7, 10, 11 (Figure 3). Thus, in calculating the equilibrium carbon dioxide generation rates, it may assumes that carbon dioxide were generated from lumps 7, 10, and 11 (Figure 4). Therefore, the values of generation rate in vector are; $m_1 = m_2 = \ldots = m_6 = m_8 = m_9 = m_{12} = 0$, and $m_7 = m_9 = m_{11} = 355$ CO_2 g/hr.

(5) State matrix, [A]. Input data of state matrix is followed by equation (5b). After constructing the state matrix [A] for different ventilation rates, the stabilities of the linear dynamic equation must be checked by calculating their eigenvalues corresponding to each state matrix (Liao and Feddes, 1990). The results show that some eigenvalues for each state matrix are negative. For example, the 12 eigenvalues of the state matrix corresponding to Q=371 m^3/hr are: 1.6, −4.9, 10.8, 7.9, 11.6, −1.3, 1.2, 9.1, 5.1 + 9.1i, and 5.1−9.1i, respectively. By a theorem on the bounded input vounded output (BIBO) stability (Decarlo, 1989), the modes of negative eigenvalues are completely unobservable. Therefore, BIBO stability rests on the boundedness of the parts of the state trajectory that are linked to the positive eigenvalues. Hence, the system are BIBO stable corresponding to each ventilation rate considered.

7. RESULTS AND DISCUSSIONS

Results for measured and calculated carbon dioxide concentrations at different ventillation rates are listed in Table 1. In concentration calculations, to convert from unit of g/m^3 to ppm (volume), it is assumed that the ideal gas law is accurated under ambient condition. The model assumed the ambeint at 30°C and 1 atm, therefore, the conversion factor for CO_2 from units g/m^3 to ppm are 560. Figure 6 shows that measured and calculated mean carbon dioxide concentration followed a similar trend for three ventilation rate levels. Table 1 also indicated that the discrepancy between measured and calculated values ranged between 8% and 13%. Figure 6 shows that the agreement between measured values and those predicted by equation (5a) is good except at lower ventilation rate, where measured carbon dioxide concentration was about 14% lower than those predicted. The reason for that may have following explanations.

(1) It is assumed that the same entrainment ratio and the same airflow patterns are used in obtaining the airflow matrices corresponding to three different ventilation rates. However, at the actual conditions the recirculation of airflow and its patterns will change in different ventilation rates. The verification results show that the air flow patterns in multiple airflow regions model better match measured results as the ventilation rate increases.

(2) Because of density difference with regard to the ambient air, the carbon dioxide concentration sets its own motion independent upon of local airflow motion. Thus, a dynamically passive carbon dioxide becomes a dynamically active gas. Therefore, transportation for an active gas is not necessary related to the airflow motion, and consequently, neither is it directly related to the flow matrix [Q] used in this model approach.

Figures 7, 8, and 9 show the transient responses of carbon dioxide concentration for measired data at three ventilation rate levels. Figures 7, 8, and 9 indicate that:

(1) Complete mixing is the best feasible operative mode for this type of ventilation system, i.e., short-circuiting system, at high ventilation rate conditions.

(2) Different points have different concentration profiles even at the same ventilation system. It seems the air movement in a ventilated airspace are turbulent and the predominant and distinctive feature of turbulence is its randomness. An inevitable consequence of the randomness is that the concentration field is also random. Therefore, the concentration field must be described in a statistical sense, i.e., in terms of mean concentration, variance, etc.

(3) Generally, the points near floor, the concentration profiles very rapidly reach their maximum concentration and then smoothly start to decay to their equilibrium concentration.

Overall, the most significant sources of error between measured and calculated values may be stated as follows.

(1) Homogenous mixing. The assumptions of local uniform mixing space and dynamically

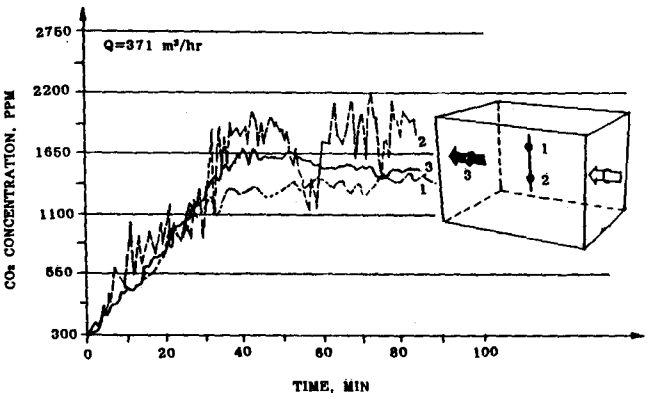

Figure 7. Transient behavior of carbon dioxide concentration at Q = 371 m^3/hr for different measuring points.

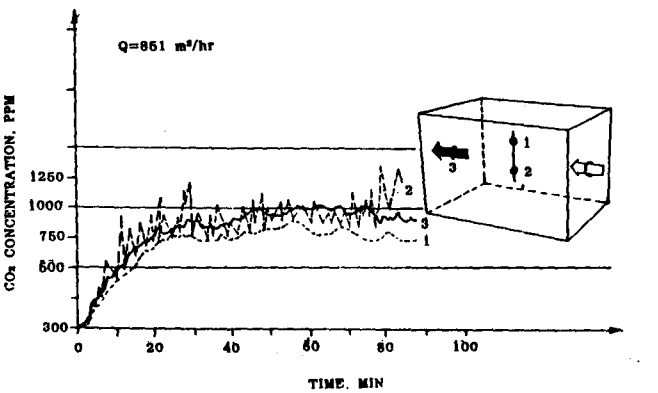

Figure 8. Transient behavior of carbon dioxide concentration at Q = 851 m^3/hr for different measuring points.

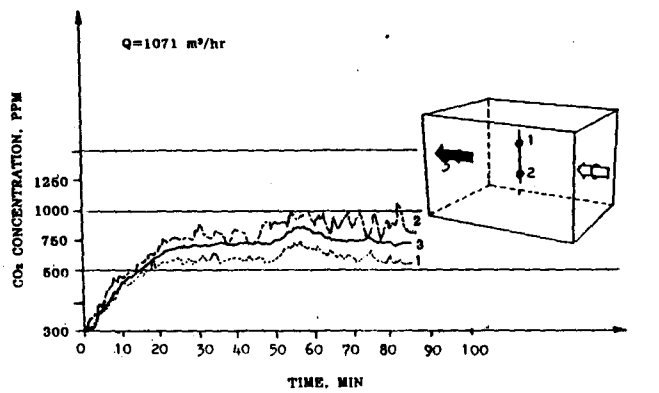

Figure 9. Transient behavior of carbon dioxide concentration at Q = 1071 m^3/hr for different measuring points.

passive carbon dioxide concentrations are used in deriving the system equations. but in the actual condition, the local convective accelerations and the density difference between carbon dioxide and air do not vanish. Therefore, any significant departure from homogeneous might be expected.

(2) Carbon dioxide generating rate. In order to investigate the effect of the error in carbon dioxide generating rate, runs were performed with the value increased by 25% and decreased by 25% (i.e., one scale of flowmeter) at the condition of ventilation rate is equal to 371 m^3/hr. The resulting changes in the measured carbon dioxide is listed in Table 1. Table 2 indicates that there is roughly a 26% – 29% change in the estimated values and the error in output is rougly equal to the error in the input in this particular case.

(3) Measured carbon dioxide concentration. (i) Zero drift: As it look for any significant error in the zero adjustment of the sampling devices to develop. Data collecting may be required for any error in zeroing to be constant over 1-4 hrs. However, adding a constant to all of the concentrations leave the linear dynamic equation (5) unchanged and so has no effect on the results. (ii) Calibrating error: The measuring device must be calibrated against a gas mixture of known carbon dioxide concentration, the concentration of the calibrating mixture may be slightly in error. Had the calibrating been perfomed, then some calibration error would have been introduced. This error causes equation (5) to read $\{ C'(t) \} = e \{ C(t) \}$ instead of $\{ C(t) \}$:

$$\{ \dot{C}(t) \} = -[A] \{ C(t) \} + 1/e[V]^{-1}$$

$$\{ m(t) \} + 1/e[D] \{ C_s(t) \} \qquad (13)$$

This has the same effect as s systematic error of 1/e in the carbon dioxide generating rate. Hence, the analysis above applies in this case. (iii) Random error: From the manufacture's specification the carbon dioxide reading to be accurate to within 3% was expected (Kasahara Chemical Instruments Crop., Japan). So random error uniformly distributed between ± 3% were applied to carbon dioxide concentration.

SUMMARY AND CONCLUSIONS

A linear control model describing the behavior of carbon dioxide concentrations undergoing local airflow transportation at any location within a ventilated greenhouse was studied from the view point of lumped parameter approximation. The ability of a lumped-parameter model predicts CO_2 concentrations at any location within a ventilated airspace based on CO_2 generation rates is also verified. The following results can be drawn from this work.

(1) The system equation of CO_2 concentration at any location within a ventilated greenhouse can be represented by a first-order vector-matrix differential equation as,

$$d \{ C(t) \}/dt = -[A] \{ C(t) \} + [V]^{-1}$$

$$\{ m(t) \} + [D] \{ C_s(t) \}, \{ C(O) \} = \{ C_o \};$$

where matrix [A] is a system state matrix, contains the essential dynamic characters of the system.

(2) The predictions of the model compared very favorably with the measured results at ventilation rate of 1071 m^3/hr (deviation was 8%), while the greatest deviation from prediction occurred at the low ventilation rates between 371 and 851 m^3/hr (13 – 14%).

(3) These deviations may arise from the carbon dioxide generating system being very sensitive to the flowmeter accuracy and the system's prediction equations being sensitive to the errors in input data or to the assumptions made in deriving the system equation.

(4) Some possible errors are: (i) Departures from homogenous mixing which is assumed in all spaces; (ii) Errors in measured CO_2 concentrations; (iii) Erros in the CO_2 generating rate. The type (i) error can be largely avoided by measuring the carbon dioxide concentration at more locations in a given space and checking that the reading do not differ significantly and by improving the quantitative and qualitative representation of airflow patterns in a ventilated airspace. The effect of errors (ii) and (iii) can be reduced to an acceptable level by improved instrumentation and procedures.

Table 1. The analysis results of carbon dioxide concentration (ppm) from the theoretical calculation and measurement in the environmental chamber experiment

sampling point	ventilation rate (m^3/hr) 1071		851		371	
	measured	cal'ed	measured	cal'ed	measured	cal'ed
1	824	909	941	1060	1785	2006
2	922	1002	1040	1168	1979	2211
3	966	1037	1080	1209	2032	2288
4	840	915	993	1067	1781	2018
5	937	1014	1042	1183	1970	2236
6	970	1043	1074	1216	1982	2300
7	1020	1090	1138	1277	2149	2403
8	982	1072	1091	1249	1977	2364
9	990	1064	1059	1240	2112	2346
10	1150	1235	1266	1439	2470	2724
11	1040	1116	1191	1300	2214	2461
12	1011	1075	1082	1253	2113	2371

Table 2. Sensitivity analysis of carbon dioxide generating rate (Q = 371 m^3/hr)

generating rate 1/min	measured mean CO_2 concen. ppm	output error %
3	2047	
4.5 (+25%)	2638	29
1.5 (−25%)	1529	26

ACKNOWLEDGEMENTS

The authors wish to acknowledge the financial support of the National Science Council of R.O.C. under grant NSC-79-0409B002-02.

REFERENCES

ASHRAE Handbook of Fundamentals. 1985. American Society of Heating, Refrigerating, and Air Conditioning Engineers. New York.

Chen, C. T. 1984. Linear system theory and design. Holt, Rinehart and Winston, Inc. New York.

DeCarlo, R. A. 1989. Linear systems. Prentice-Hall, Ins., Englewood Cliffs, New Jersey.

Hadley, G. 1961. Linear Algebra. Addison-Wiley, Reading, Mass.

Himmelbalu, D. M., and K. B. Bischoff. 1968. Process analysis and simulation. Deterministic systems. John Wiley and Sons, New York.

Landau, L. D., and E. M. Lifshitz. 1987. Fluid mechanics. 2nd ed. Pergamon Press, New York.

Liao, C. M., and J. J. R. Feddes. 1990. Mathematical analysis of a lumped-parameter model describing the behavior of airborne dust in animal housing. Applied Math. Modelling, 14: 248-257.

Liao, C. M., T. S. Wang, and C. M. Liu. 1991. A lumped-parameter model describing the behavior of carbon dioxide concentrations in a slot-ventilated airspace. Part II: Model verification. J. of the Society of Agricultural Structures, Japan. (Accepted)

Monteith, J. L. 1963. Gas exchange in plant communities. *In* Environmental Control of Plant Growth, ed. L. T. Evans. Academic Press, New York.

Noggle, G. R., and G. J. Fritz. 1976. Introductory plant physiology. Prentice-Hall, New Jersey.

Plemmons, R. J. 1977. M-matrix characterizations. I – Nonsingular M-matrices. Linear Algebra and its applications, 18: 175-188.

Saffell, R. A., and B. Mattewa. 1983. Computer control of air-temperature in a glasshouse. J. Agric. Eng. Res. 28:469-477.

Kasahara Chemical Instruments Crop. 1989. User's Guide for KRK Model 200-type CO_2 Meter, Saitma, Japan.

收稿日期：民國80年 2月 7日
修正日期：民國80年 3月 4日
接受日期：民國80年 3月15日